

Final Technical Report

ACTIVE DEFORMATION AND EARTHQUAKE POTENTIAL OF THE SOUTHERN LOS ANGELES BASIN, ORANGE COUNTY, CALIFORNIA

Award Number: 01HQGR0117

Recipient's name: University of California - Irvine
Sponsored Projects Administration
160 Administration Building, Univ. of CA - Irvine
Irvine, CA 92697-1875

Principal investigator: Lisa B. Grant, Ph.D.
Department of Environmental Analysis & Design
262 Social Ecology 1
University of California
Irvine, CA 92697-7070

Program element: Research on earthquake occurrence and effects

Research supported by the U.S. Geological Survey (USGS), Department of the Interior, under USGS award number 01HQGR0117. The views and conclusions contained in this document are those of the authors and should not be interpreted as necessarily representing the official policies, either expressed or implied, of the U.S. Government.

Award number: 01HQGR0117

ACTIVE DEFORMATION AND EARTHQUAKE POTENTIAL OF THE SOUTHERN LOS ANGELES BASIN, ORANGE COUNTY, CALIFORNIA

Eldon M. Gath, University of California, Irvine, 143 Social Ecology I, Irvine, CA, 92697-7070; tel: 949-824-5382, fax: 949-824-2056, email: egath@uci.edu

Eric E. Runnerstrom, University of California, Irvine, 143 Social Ecology I, Irvine, CA, 92697-7070; tel: 949-824-5382, fax: 949-824-2056, email: erunners@uci.edu

Lisa B. Grant (P.I.), University of California, Irvine, 262 Social Ecology I, Irvine, CA, 92697-7070; tel: 949-824-5491, fax: 949-824-2056, email: lgrant@uci.edu

TECHNICAL ABSTRACT

The Santa Ana Mountains (SAM) are a 1.7 km high mountain range that form the southeastern boundary of the Los Angeles basin between Orange and Riverside counties in southern California. The SAM have three well developed erosional surfaces preserved on them, as well as a suite of four fluvial fill terraces preserved in Santiago Creek, which is a drainage trapped between the uplifting SAM and a parallel Loma Ridge. By correlation of the terraces with the marine eustatic sea level curve, we were able to estimate a 0.31 mm/yr uplift rate for the SAM and an emergence age of ~3.6 Ma. Using a new method for temporally quantifying the age of drainage basins, we were able to develop an alternative check of the age of the SAM. This methodology was first developed in the adjacent Puente Hills by developing a correlation between basin area and basin age. The basin age was calculated by measuring the right-lateral strike-slip displacement of each basin's primary stream, and regressing it against the basin's area. Because the Whittier fault's slip rate is known (2.5 mm/yr), the age of the channel can be calculated by retrodeforming it. From this analysis, the Puente Hills have been rising 0.4 mm/yr since their emergence 700-1,200 ka. Santiago Creek formed ~2.4 Ma in conjunction with the initiation of the Loma Ridge structure, a parasitic structure that formed in response to compressional buckling of sedimentary strata on the flanks of the uplifting Santa Ana block. Hanging wall block faulting appears to have deflected Santiago Creek northerly ~1,200 m along five discrete block margin faults. The source of this strain is still undetermined, though it may be from the same north-vergent structures that are generating the San Joaquin Hills uplift. The termination of the Elsinore fault into the Chino and Whittier faults leaves at least 1-2 mm/yr of north-vergent strain unaccounted. We speculate that this strain is being transferred into uplift of the SAM, with complex interaction among other north-vergent structures in southern California.

NON-TECHNICAL ABSTRACT

The Santa Ana Mountains are prominent features in the landscape of the metropolitan Los Angeles basin. Comparable sized mountains and foothills in surrounding areas are known to be associated with active faults or folds. This project investigates possible tectonic deformation and earthquake potential associated with undiscovered faults in or near the Santa Ana Mountains by examining the patterns carved into the landscape by streams. Preliminary results suggest that the mountains are rising at a rate of approximately 0.3 mm/yr and may contain active faults.

INTRODUCTION

Rising to a height of over 1,700 meters above sea-level, the Santa Ana Mountains (SAM) are the northernmost extent of the California Peninsular Ranges (Figure 1) at the southeast margin of the Los Angeles basin (Figure 2). They rise nearly 900 meters above the heavily populated urban centers in Orange and Riverside Counties, but neither their uplift rate nor uplift mechanism has been determined. The SAM are the dominant landform in southern Orange and western Riverside County, yet they have not been included in seismic hazard models. This research presents an initial geomorphic analysis of the SAM designed to quantitatively understand the spatial and temporal pattern of deformation as a first step towards quantifying the seismic hazard.

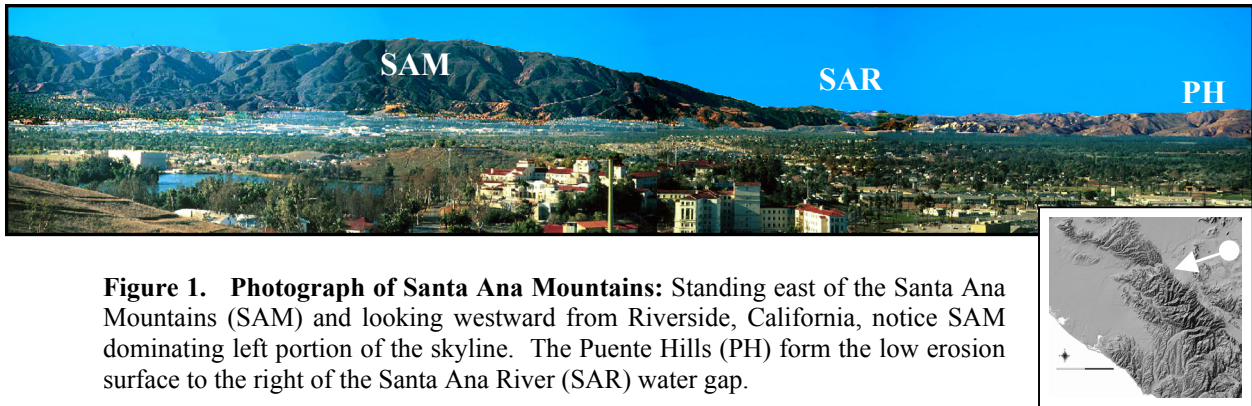


Figure 1. Photograph of Santa Ana Mountains: Standing east of the Santa Ana Mountains (SAM) and looking westward from Riverside, California, notice SAM dominating left portion of the skyline. The Puente Hills (PH) form the low erosion surface to the right of the Santa Ana River (SAR) water gap.

The principal goal of this study was to develop a broad understanding of the nature of the SAM uplift, and to begin integrating these findings into the general seismic hazard framework of southern Los Angeles basin in Orange County, southern California. There is a constant, dynamic interaction between the tectonic forces acting to uplift a mountain range and the fluvial and erosive forces acting to lower a mountain range (Pazzaglia et al., 1998). The pattern and growth of a drainage network has been long recognized as one of the most sensitive indicators of tectonic deformation (Hack, 1973; Schumm, 1986). On this basis, we mapped and quantitatively analyzed the geomorphology of the drainage system to understand the temporal pattern of uplift of the SAM.

The area of study is dominated by the SAM (Figure 2), but there are many other geomorphic features of significance. Tables 1 and 2 present a summary of these geomorphic and structural features, as well as a description of their relationship to the tectonic geomorphology of the SAM.

METHODOLOGY

Fluvial network analysis

Many studies have demonstrated that examination and analysis of fluvial system development patterns can be applied to quantify neotectonic deformation (e.g., Ohmori, 1993; Montgomery, 1994; Nicol et al., 1994; Kirby and Whipple, 2001). Profiles of channels and elevated terraces contain information about deformation rates and patterns. In a study to determine the rate of regional uplift, Merritts et al. (1994) mapped the long channel profiles of elevated fluvial terraces

to determine the evolution of the channel profile, also referred to as “grade,” through time. Cox (1994) used an asymmetric pattern of drainage system evolution as a proxy to indicate the regional tilting and tectonic deformation. Bullard and Lettis (1993) mapped elevated geomorphic surfaces and a pattern of channel abandonment to reveal subsequent deformation in order to model the pattern of uplift by a localized blind thrust fault. Rosenbloom and Anderson (1994) measured longitudinal channel profiles of rivers cut through elevated marine terraces on a progressively uplifting mountain range to correlate residual river knickpoints with marine terrace elevations. This indicated that bedrock channels fail to fully regrade after pronounced base level lowering, and thus preserve a record in their longitudinal profile of the eustatic cycles to which they have been subjected. Unfortunately, neither the Santa Ana River nor the Santiago Creek have consistent terraces from which to construct long-channel terrace profiles.

For our initial analysis, we examined the relationship between drainage basin area and time in the evolutionary development of a fluvial network. This approach has not been widely applied at a regional scale primarily because of the difficulty in providing temporal control for the drainage basins. Our study overcame this difficulty by developing and applying empirical relationships between drainage basin area and age. The relationships were derived in the Puente Hills, where the Whittier fault has a known slip-rate (e.g., Gath et al., 1992). Gath (1997) measured right-lateral displacements across the fault that were consistent, long-term, and tectonic. Therefore, starting in the Puente Hills, we first derived a relationship between basin area and channel displacement. Next, we determined a relationship between basin area and main-channel age by dividing channel offset by the lateral slip rate of the fault, yielding a formula for basin age as a function of basin area. Finally, we applied this formula for basin age to the Santiago Creek drainage basin in an attempt to determine an approximate emergence age for the SAM.

In order to check the age estimation for Santiago Creek, we also mapped fluvial fill terraces and geomorphic strath surfaces on both the Puente Hills and SAM. These terraces were correlated to the marine eustatic sea level curve used by Grant et al. (1999) to measure the uplift rate and emergence of the San Joaquin Hills. This independent measure of emergent age was consistent with the age derived by drainage basin initiation.

Computational methods

We automated our process for characterizing and analyzing drainage basins, fluvial networks, and topography by using computer software. We used both RiverTools v2.4 (a product of Rivix, LLC, and supported by Research Systems, Inc.) and ArcView v3.2a (a product of Environmental Systems Research Institute) on a Windows2000 workstation. RiverTools was used to patch, also known as “to mosaic,” together USGS 7.5-minute digital elevation models (DEM); to delineate drainage basin boundaries based on user-specified basin outlet points; and to derive river networks, as well as to derive empirical characteristics of those networks. ArcView was used to map RiverTools' output in a geographic information systems (GIS) format; to layer datasets; to create figures; to generate 3D oblique landscape perspectives of our study area; and to derive ridge-top profiles.

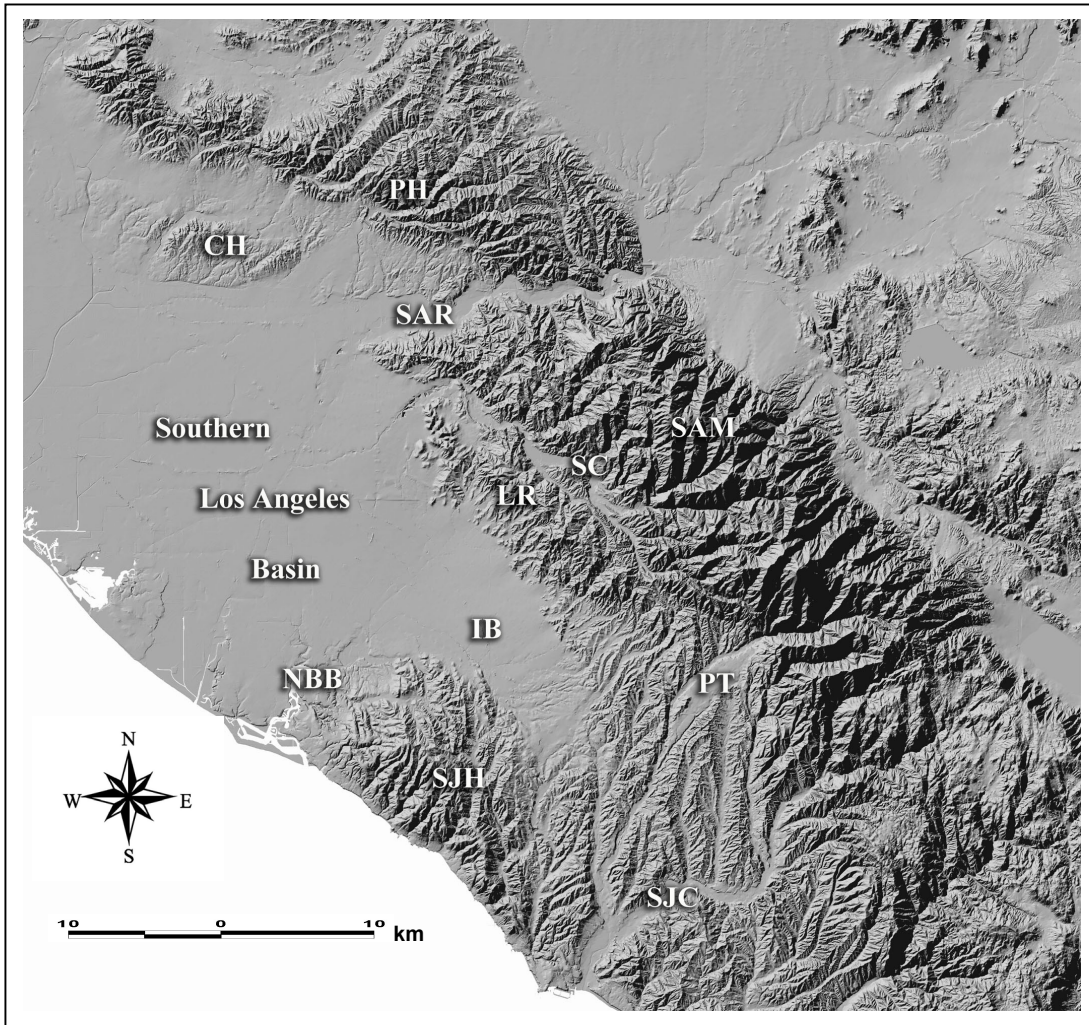


Figure 2. Location map: Shaded digital elevation model of the southern Los Angeles basin, which encompasses Orange County, showing locations and physiography of the study area described in this report. Abbreviations are as follows: Santa Ana River (SAR), Puente Hills (PH), San Joaquin Hills (SJH), Loma Ridge (LR), Santiago Creek (SC), Irvine Basin (IB), Coyote Hills (CH), Newport Back Bay (NBB), Plano Trabuco (PT), San Juan Creek (SJC), and Santa Ana Mountains (SAM).

We patched together 38 USGS native-format DEMs to build the geographic coverage for our study area and vicinity. Coverage of individual DEMs represents the same geographic extent as USGS 7.5-minute quadrangles by the same name. The DEMs were georeferenced to the North American Datum of 1927, Universal Transverse Mercator projection, zone 11 north. See Appendix for a complete listing of quadrangle names. DEM coverage of the Puente Hills required portions from 7 quadrangles; each had 10 m horizontal resolution with elevation units in feet. DEM coverage of the SAM required portions from 11 quadrangles; each had 10 m horizontal resolution with elevation units in feet, except for the Corona North quadrangle, which had elevation in meters.

Table 1. Local landforms: Significant physiographic features in the geomorphic evolution of the southeast Los Angeles basin, Orange County, California.

Feature	Description and Significance
Santa Ana Mountains	The SAM are a Peninsular Ranges mountain chain, cored by granitic rocks of the southern California batholith. They extend northward from San Diego County to the Santa Ana River; rising over 800 m above the river, to an elevation of 1750 m. They are bounded on the east by the Elsinore fault, and are overlapped by Santa Ana River sediments on the west. The northern end of the range exposes a south-dipping Cretaceous through Miocene sedimentary sequence.
Puente Hills	The Puente Hills are an anticlinal structure that expose deformed Miocene sedimentary rocks, predominantly of the Puente Formation. They are bounded between the Santa Ana River on the southeast and the San Gabriel River on the northwest, and extend from San Jose Creek on the north to the Chino basin on the east. They rise over 360 m above the Los Angeles basin to an elevation of 460-540 m. The southern flank is mantled by Quaternary sediments of the Santa Ana and San Gabriel river and is traversed by the dextral, strike-slip Whittier fault. They have a well-developed, southerly-draining, fluvial network that has been pervasively and right-laterally deformed by the lateral slip on the Whittier fault. This drainage network has formed an alluvial fan apron along the southern flank of the Puente Hills. A blind thrust ramp is proposed as an uplift mechanism (Shaw and Shearer, 1999).
Coyote Hills	The Coyote Hills are an anticlinally folded sequence of Quaternary sediments that have been elevated 160-180 m above the surface of the Santa Ana River sedimentary basin. The Coyote Hills are separated into an East and a West structure by Brea Creek. Both of the folds are also traversed by several wind gaps. The Coyote Hills sedimentary sequence includes the San Pedro Formation of ~700 ka, the Coyote Hills Formation of ~200-400 ka, and the La Habra Formation of ~100-200 ka. Similar anticlinal structures lie both east and west of the Coyote Hills. While the uplift structure has been modeled (Shaw and Shearer, 1999), the uplift rate is not well quantified.
San Joaquin Hills	The San Joaquin Hills have been uplifting at a rate of 0.25 mm/yr for at least 1 Ma by a northeast vergent blind thrust fault. They are ringed by elevated shorelines from which the uplift rate and structure were modeled (Grant et al., 1999). Several of the many vertical faults that cut through the hills have been observed to displace older terraces, but these faults have been confirmed to all be older than Holocene, and most are older than Stage 5e. The southern extent of the San Joaquin Hills uplift is still poorly constrained. Rivero et al. (2000) link the San Joaquin Hills uplift to the offshore Oceanside thrust.
Loma Ridge	Loma Ridge is the crest of the Irvine Foothills, composed of a late Cretaceous through early Pleistocene sedimentary sequence on the western flank of the SAM. The sediments have been extensively deformed by folding and faulting, up to 80° dips in Pleistocene beds (Morton and Miller, 1981). Loma Ridge is separated from the SAM by Santaigo Creek, a northwesterly flowing river that has been consistently deformed ~1,200 m north by each of 5 north-trending en-echelon faults cutting through the sedimentary section of Loma Ridge. The crest of Loma Ridge has at least four topographic steps decreasing in elevation westerly.
Santa Ana River	The Santa Ana River is a primary trunk stream that drains the San Bernardino Mountains, through the Prado/Chino basin and the Santa Ana Canyon water gap, before finally discharging into the Pacific Ocean at Huntington Beach. The Santa Ana River drains an area of 4400 km ² . It has been proposed that the Santa Ana River is antecedent to the Puente Hills-SAM uplift (Mendenhall, 1905). This hypothesis has never been tested.

Feature	Description and Significance
Santiago Creek	Northwestward flowing Santiago Creek is pinned between the SAM and the Loma Ridge structures before finally joining with the Santa Ana River. It may have been deflected northward (upstream) by five north-trending block faults. Terraces are present along the length of Santiago Creek, but they have never been mapped in detail nor correlated. Santiago Creek appears to be antecedent to the growth of Loma Ridge, and progressively deflected westerly as Loma Ridge grows westerly. Two wind gaps are present through the El Modena/Jamboree/Tustin area which are speculated to have been ancestral courses of Santiago Creek as it was progressively deflected westward to the Santa Ana River. The Jamboree/Tustin wind gap is speculated to be the course of Santiago Creek when it cut the Newport Back Bay channel.
Trabuco Canyon Plano Trabuco	The Plano Trabuco is one of the most striking geomorphic features of southern Orange County. It is a gently dipping, 2 km wide, alluvial fill terrace, stretching 10 km southwestward from the SAM range front. The terrace is truncated at the north-trending Cristianitos fault. Trabuco Canyon today is underfit as a source of Plano Trabuco.
San Juan Creek	San Juan Creek is the largest river in southern Orange County. It drains southwesterly from the SAM into the Pacific Ocean at Dana Point. It has a trellis shaped tributary system of north-trending drainages that are obviously structurally controlled, but by an undefined structure. San Juan Creek is deformed where it crosses the Cristianitos fault. One north-trending tributary of San Juan Creek has captured the Trabuco Canyon drainage, and also the Oso Creek drainage, both formerly flowing through the San Joaquin Hills to the Pacific.

Basins are basic landscape units that are bounded by a drainage divide and occupied by a drainage system. They are distinguished according to an area across which all flow collected in their interior exits the basin across a narrow segment called a basin outlet, sometimes referred to as the mouth of the basin or canyon. Lower-order basins may be nested within higher-order basins. Basins, by definition, have only one outlet.

We hand-picked the basin outlets. After using software to derive river networks in the Puente Hills and SAM, we layered the river networks over the patched DEM in order to review the locations and magnitudes of fluvial channels relative to the topography. Within the SAM, basin outlets were identified to be those points nearest the mouths of mutually exclusive canyons, along higher-order streams, immediately upstream of the point of junction with the SAM's highest-order stream channel (Santiago Creek). Within the Puente Hills, basin outlets were identified to be those points nearest the mouths of mutually exclusive canyons, where higher-order streams intersected the geomorphic expression of the Whittier fault trace. For each user-specified basin outlet, we used RiverTools to extract basin boundaries based on the river network and elevation data embedded with the DEMs.

Additional data from other studies within the vicinity of our study area were used to expand our quantitative understanding of the geomorphic evolution of the SAM. These other studies, described in the next section, examined the San Joaquin Hills (see Grant et al., 1999) and the Puente Hills (see Gath, 1997).

Table 2. Local faults: Faults in the geomorphic evolution of southeast Los Angeles basin, Orange County, California.

Structural Feature	Kinematics	Slip Rate	Discussion	References
Elsinore fault	Right-lateral strike-slip N45-50°W 45-90°SW	4-6 mm/yr	Extends from Mexico border to San Gabriel River, and possibly to the Hollywood Hills. Primary strain contributor to eastern Los Angeles basin.	Lamar and Rockwell, 1986; Petersen and Wesnousky, 1994
Whittier fault	Right-lateral strike-slip N65-70°W 70°NE	2-3 mm/yr	Northern segment of the Elsinore fault, extending between the Santa Ana and San Gabriel rivers. Paleoseismic trenching produced slip rate from dated, displaced, fluvial piercing points. Displacements at least 10h:1v.	Durham and Yerkes, 1964; Yerkes, 1972; Gath et al., 1992; Rockwell et al., 1992; Gath, 1997.
Chino fault	Reverse slip (west side up) N10°W, dips SW	0.5-1.5 mm/yr	Splays off of the Elsinore fault about 16 km south of the Santa Ana River. Displaces late Quaternary alluvial sediments in the Prado Dam area of the Santa Ana River. Assumed to be a steeply west-dipping reverse fault with little lateral displacement, but is probably dominantly right-lateral strike slip.	Gray, 1961; Weber, 1977; Heath et al., 1982
Cristianitos fault	Normal?	N/a	Cuts north-south up Cristianitos Canyon from San Clemente to Santiago Creek north of El Toro. Generally considered to form the southern extensional boundary of the Capistrano Embayment. Appears to deform San Onofre Creek, Trabuco Creek, and Santiago Creek. Activity stated to be pre-Stage 5e based on marine terrace exposure.	Morton and Miller, 1981; Ryan et al., 1982
El Modena fault	inconclusive	N/a	Cuts north-south up the abandoned wind gap of Santiago Creek. Offsets the El Modena volcanic rocks against the sedimentary sequence of Loma Ridge. Inconclusive evidence for activity – reports of offset modern surface soils, also reports of 20+ ky terraces not offset.	Morton and Miller, 1981
Peralta Hills fault	Reverse slip (north side up) Strikes east-west, dips shallowly N	N/a	Trends along the base of Burruel Ridge on the eastern side of the Santa Ana River. It is a low-angle reverse fault that displaces Miocene bedrock over elevated stream terrace gravels of Santiago Creek. Latest Quaternary-Holocene offset of colluvial deposits by a lateral-slip, hanging wall fault.	Schoellhamer et al., 1981; Bryant and Fife, 1982; Whitney and Seymour, 1992
Norwalk fault Puente Hills fault	Reverse slip (north side up) N 65-85° W	N/a	Mapped as a subsurface fault along the southern margin of the east and west Coyote Hills based on oil well logs. Speculated as an extension of the Peralta Hills fault, and may have generated the 1929 M 4.7 “Whittier” earthquake. Surface expression of the Norwalk fault is unknown. Recently renamed Puente Hills fault by Shearer and Shaw (1999).	Yerkes, 1972; Bryant and Fife, 1982; Shaw and Shearer, 1999

San Joaquin Hills terrace correlations

Carved onto the south and western flank of the San Joaquin Hills is a suite of eight marine terraces (Figure 3). These terraces were mapped, dated, and correlated to the marine eustatic sea level curve by Grant et al. (1999). An emergence age of ~1.4 Ma was estimated for the San Joaquin Hills based on an uplift rate of 0.25 mm/yr calculated from a coral dated at 122 ka, assuming that the uplift rate was consistent across time (Grant et al., 1999). The correlation between uplifted geomorphic surfaces and the marine eustatic sea level curve established a local marine terrace chronology.

The San Joaquin Hills data are useful for our study of the SAM because they allow us to correlate marine surfaces on the inland side of the San Joaquin Hills with potentially equivalent marine surfaces on the foothills of Loma Ridge. As shown on Figure 3, marine terraces were established on the northern extent of the San Joaquin Hills between 200-500 ka. Shorelines along the base of Loma Ridge would be older than 200-300 ka given our assumptions as follows: the Irvine Basin (Figure 2) between the San Joaquin Hills and the Loma Ridge area was subaerial after ~200-300 ka; given eustatic highstands, the Irvine Basin was too shallow to generate shorelines that are preserved in the geomorphology. This assumption is supported by the apparent absence of marine shorelines on the inland (northeast) side of the San Joaquin Hills.

We applied the San Joaquin Hills marine terrace correlation data to a series of six fill terraces and strath surfaces in the Puente Hills, and to eight similar surfaces newly mapped in the northwestern section of the SAM. This application of marine eustatic sea level curves allowed us to constrain temporal uncertainties regarding the age of geomorphic surfaces within the SAM.

RESULTS

Puente Hills drainage basin age and area

All Puente Hills streams that cross the Whittier fault are right-laterally deflected by distances varying from 4 m to 1,675 m (Gath, 1997). Gath proposed that the stream deflections were caused by repeated coseismic displacements across the strike-slip Whittier fault. Drainage basins enlarge predictably over time based on slope, geology, and climate (Schumm et al., 1987). Consequently, a strong relationship between drainage basin area and time should exist in the Puente Hills because right-lateral displacements are temporally based. To confirm this, we calculated the areas of the drainage basins and regressed them against displacement measured by Gath et al. (1997).

We used measurements of right-lateral displacements across streams bisected by the Whittier fault as a proxy for the age of the initiation of the discrete drainage basins in the Puente Hills. Age was calculated to be the measured displacement divided by the fault slip-rate that was reported in a previous paleoseismic investigation (see Gath et al., 1992). By reconstructing the history of right-lateral stream displacements, we identified the correlation between drainage basin area and drainage basin age. This relationship was then applied to the Santiago Creek drainage basin in the SAM to provide a first order approximation of the age of the basin, and thus a second independent way to estimate the age of the SAM.

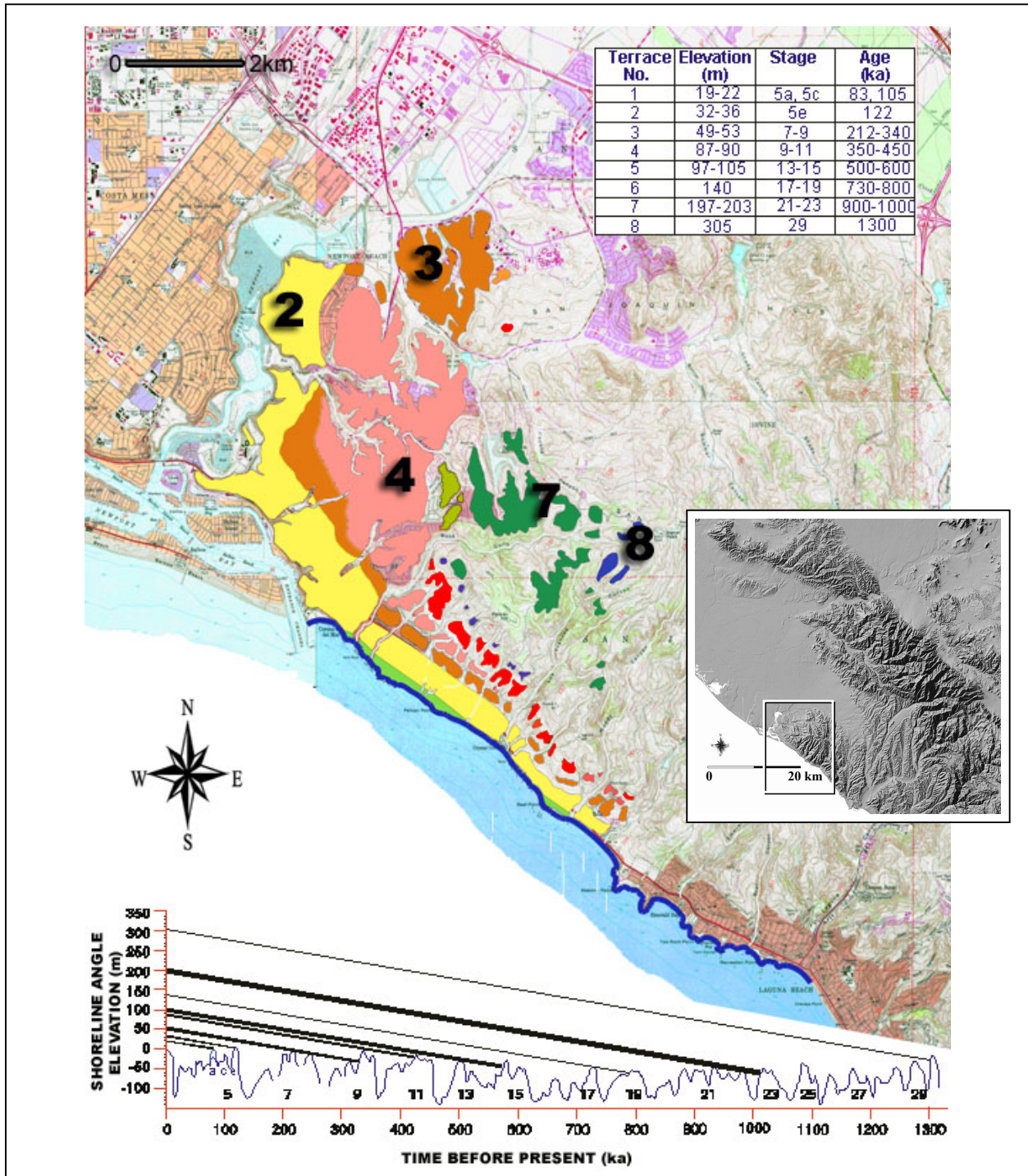


Figure 3. Marine terraces in the San Joaquin Hills: Marine terraces are shown in color, layered over a topographic base-map of the northwestern San Joaquin Hills. The shoreline elevation age and corresponding marine oxygen isotope stage is summarized in inset table. Ages were measured directly by dating corals and were estimated by correlating with sea-level highstands as shown in lower chart. Figure is modified from Grant et al. (1999).

Using RiverTools, we identified and measured the area of fourteen drainage basins in the Puente Hills, all of which exhibited offset of the primary stream by the Whittier fault. Because one of the variables in the growth of the basin area is climate, it was necessary to use only those basins old enough to have experienced several climatic cycles. For this analysis, we only used drainage basins where the measured displacement exceeded 250 m.

The rate of slip on the Whittier fault was determined by Gath et al. (1992) to be 2.5 ± 0.5 mm/yr based on a detailed 3D trenching study. The stream displacements are directly linked to the slip rate, meaning that it is possible to regress drainage basin area against age. Dividing the offset by the rate of slip yields the drainage basin age. All of the drainage basins are within the Puente Formation, which is a Miocene marine unit composed of well-bedded sandstones, shales, and rare conglomeratic units (Yerkes, 1972). At the general and regional scale of this analysis, all of the measured drainages have the same bedrock lithology and are not likely to be affected by local durability variations in the bedrock.

Table 3. Fourteen drainage basins in the Puente Hills: area, offset, and age

Basin	Name	Area (km ²)	Offset (m)	Age (ka)
A	Brea	15.9	1372	549
B	Tonner	23.7	1676	670
C	Olinda a	1.0	305	122
D	Olinda landfill	0.9	248	99
E	Olinda b	1.4	419	168
F	Carbon	24.0	1676	670
G	Telegraph	8.5	457	183
H	unnamed	2.8	548	219
I	Yorba Linda	0.7	411	164
J	Blue Mud	2.6	366	146
K	Lomas de Yorba	0.7	351	140
L	Box	1.3	396	158
M	Bee	2.2	381	152
N	Bryant	0.5	259	104

Using a 2.5 mm/yr right-lateral slip rate (Gath et al., 1992) along the Whittier fault, Gath (1997) reported age, based on tectonic offset, for drainage basins in the Puente Hills. Drainage basin area (this study) is then correlated to offset and age to derive an empirical relationship (Figures 5, 6).

Figure 5 illustrates the strong relationship between growth of the drainage basin through time, and the cumulative displacements of the channel by recurrent earthquakes on the Whittier fault. Figure 6 transforms the displacements into channel age, thereby producing a basin area growth rate that can be used in the Loma Ridge area where the Tertiary sedimentary units are lithologically similar to the Puente Formation in the Puente Hills (Morton and Miller, 1981).

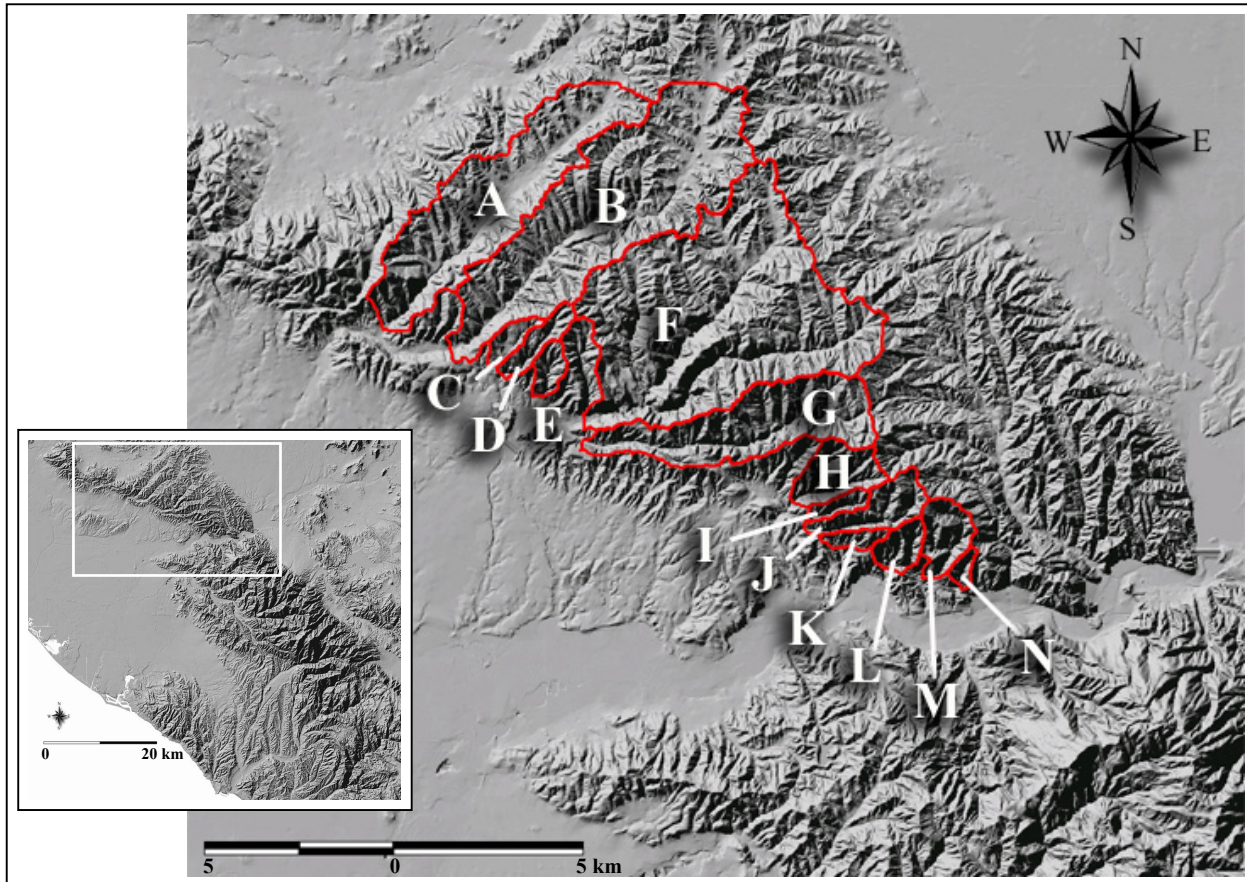


Figure 4. Puente Hills drainage basins: DEM of the Puente Hills showing the consistent right-lateral offset of all Whittier fault-crossing streams in the Puente Hills. The fourteen drainage basins (A-N) used in the regression analysis are outlined in red.

Geomorphic mapping by Gath (1997) revealed three fill and three strath terraces on the Puente Hills within the Santa Ana River canyon. Pedogenic profile descriptions on the two lowest fill terraces yielded ages of approximately 80 ka and 120 ka (Rockwell et al., 1988). Correlation with the same eustatic sea level curve as Grant et al. (1999), yielded an uplift rate of 0.4 mm/yr, and an emergence age of ~1 Ma for the Puente Hills (Figure 7). The largest drainage basins (Carbon, Tonner, and La Mirada) in the Puente Hills are all offset about 1,700 m (Gath, 1997). Using the Gath et al. (1992) slip rate of 2.5 mm/yr, these drainages incised ~700 ka, which is consistent with the age of the second geomorphic surface estimated by correlating with sea-level highstands (Figure 3). Gath (1997) also interpreted 2,700 m of deflection on the Santa Ana River and ~3,000 m of deflection on the San Gabriel River. Based on the 2.5 mm/yr slip rate, the age for the entrainment of these two trunk streams within the emerging Puente Hills is ~1,100-1,200 ka, which is consistent with the age extrapolated from the sea level correlation chart for the oldest erosional surface on the Puente Hills (Figure 7).

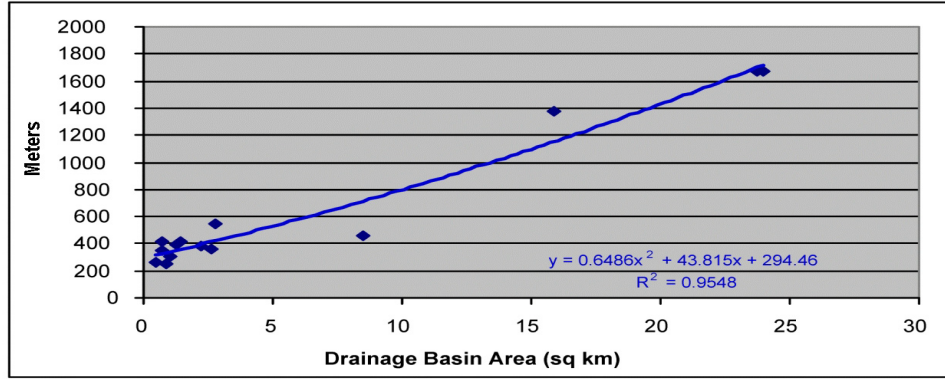


Figure 5. Puente Hills, displacement vs. area: Regression plot of the drainage basin area (km^2) against the cumulative displacement (m) of the main stream across the Whittier fault based on data in Table 3; correlation coefficient $R^2 = 0.95$.

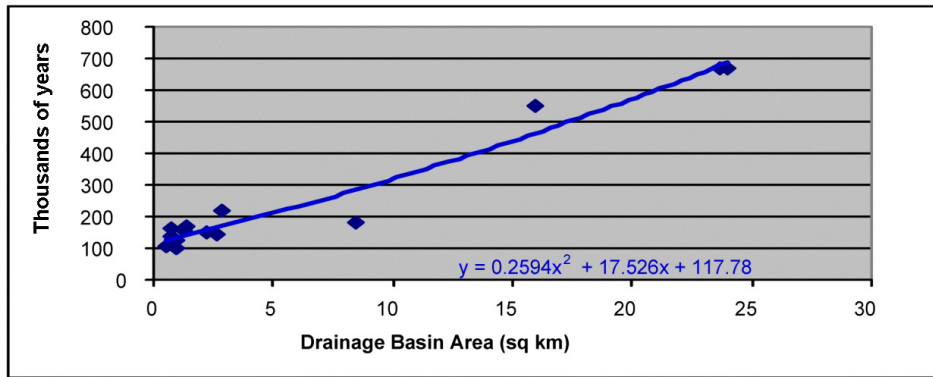


Figure 6. Puente Hills, age vs. area: Regression plot of the drainage basin area (km^2) against the age of the basin (thousands of years). The age was calculated by dividing the cumulative fault displacement by the rate of slip of the fault, yielding initial age of incision. Because it is only a numerical transformation, the R^2 correlation coefficient remains the same, although the formula is different.

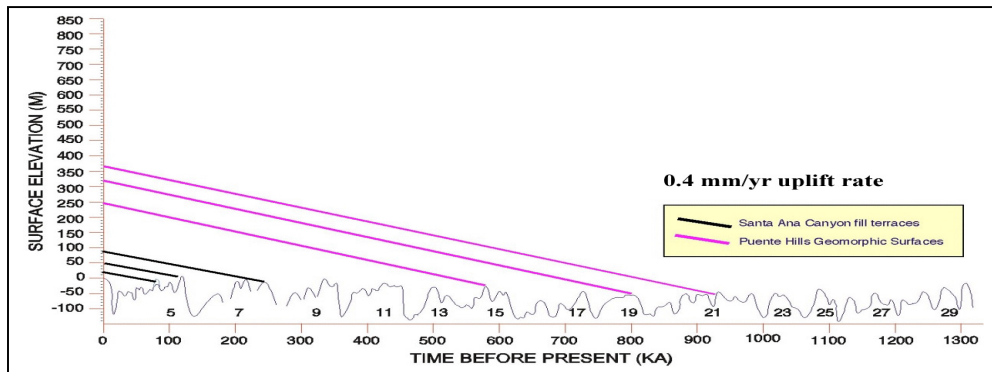


Figure 7. Puente Hills geomorphic surfaces, elevation vs. eustatic sea level: Uplift rate plot of fluvial terraces derived from the six fill and strath terraces mapped in the Puente Hills (Santa Ana River canyon) (Gath, 1997). Ages of the three youngest terraces were estimated from soil profile development, then correlated to the eustatic sea level curve used in the San Joaquin Hills by Grant et al. (1999). We calculate the uplift rate to be 0.4 mm/yr and an emergence age of ~1 Ma.

Santa Ana Mountains

We identified eight discrete geomorphic surfaces on Loma Ridge and the SAM (see four highest surfaces in Figure 9). These are interpreted to be erosional surfaces created during past eustatic high stands, similar to those in the San Joaquin and Puente Hills. Episodic uplift of the SAM can be calculated based on correlation with the eustatic sea level curve, assuming two factors: (1) the uplift rate is constant, and (2) the lowest surface corresponds to marine oxygen Isotope Stage 7-9. Constant uplift must be assumed in the absence of datable deposits. A Stage 7-9 age for the 70 m surface is approximately equivalent to the lowest shoreline or erosional surface identified at the toe of Loma Ridge (see green line on Figure 9). This age is also consistent with the inferred closing of the embayment from previous studies of the San Joaquin Hills (e.g., Grant et al., 1999). The four lowest fluvial fill terraces (not shown in Figure 9) inset within Santiago Creek are graphed on Figure 10 as light-red lines.

The erosional surfaces give Loma Ridge a stepped appearance, consistently lower to the west (see Figure 9). We interpret Loma Ridge to be a north-vergent structure consistently deforming Santiago Creek to the west by ~1,200 m between growth steps.

The Santiago Creek basin drains nearly the entire SAM north of Trabuco Creek (Figure 8). It can be divided into eight sub-basins, ranging in size from 8 km² to 49 km² (Table 4). Based on geologic mapping by Morton and Miller (1981), three of the basins are formed within batholithic granitic and metamorphic rocks that form the core of the SAM; the other five basins are formed in Cretaceous to Miocene sedimentary rocks. All of the Santiago Creek watershed bedrock units are older and more lithified than the Puente Formation of the Puente Hills. Nevertheless, there should still be a time-dependent relationship to the areal expansions of the basins. Applying the same basin age-basin area equation from the Puente Hills is a first step towards estimating the age of formation of the Santiago Creek drainage.

Climate, geology, slope, and time are the most critical factors in basin development. The SAM stand twice as tall as the Puente Hills, thereby providing an increased precipitation source that would accelerate basin development more rapidly than the Puente Hills development rate. The bedrock units of the SAM are older, more lithified, and presumably more resistant to erosion than the Puente Hills, thereby retarding the development rate. However, both basins have experienced similar climatic fluctuations, and both are approximately equal distances from the coast. In summary, it seems appropriate to compare the ages of the Santiago Creek drainage basins with the Puente Hills basins using the same regression equations derived from the Puente Hills, as long as the differences between them are clear.

Based on Figure 11, which combines areas for basins GG and HH, the initiation of the Santiago Creek drainage appears to have commenced ~2.4 Ma. This age is consistent with Hull and Nicholoso's (1992) estimate of the maximum age of the Elsinore fault (~2.5 Ma) on the northeast side of the SAM. The ~2.5 Ma age is derived from the age of the Temecula Arkose formation deposited in the Temecula trough.

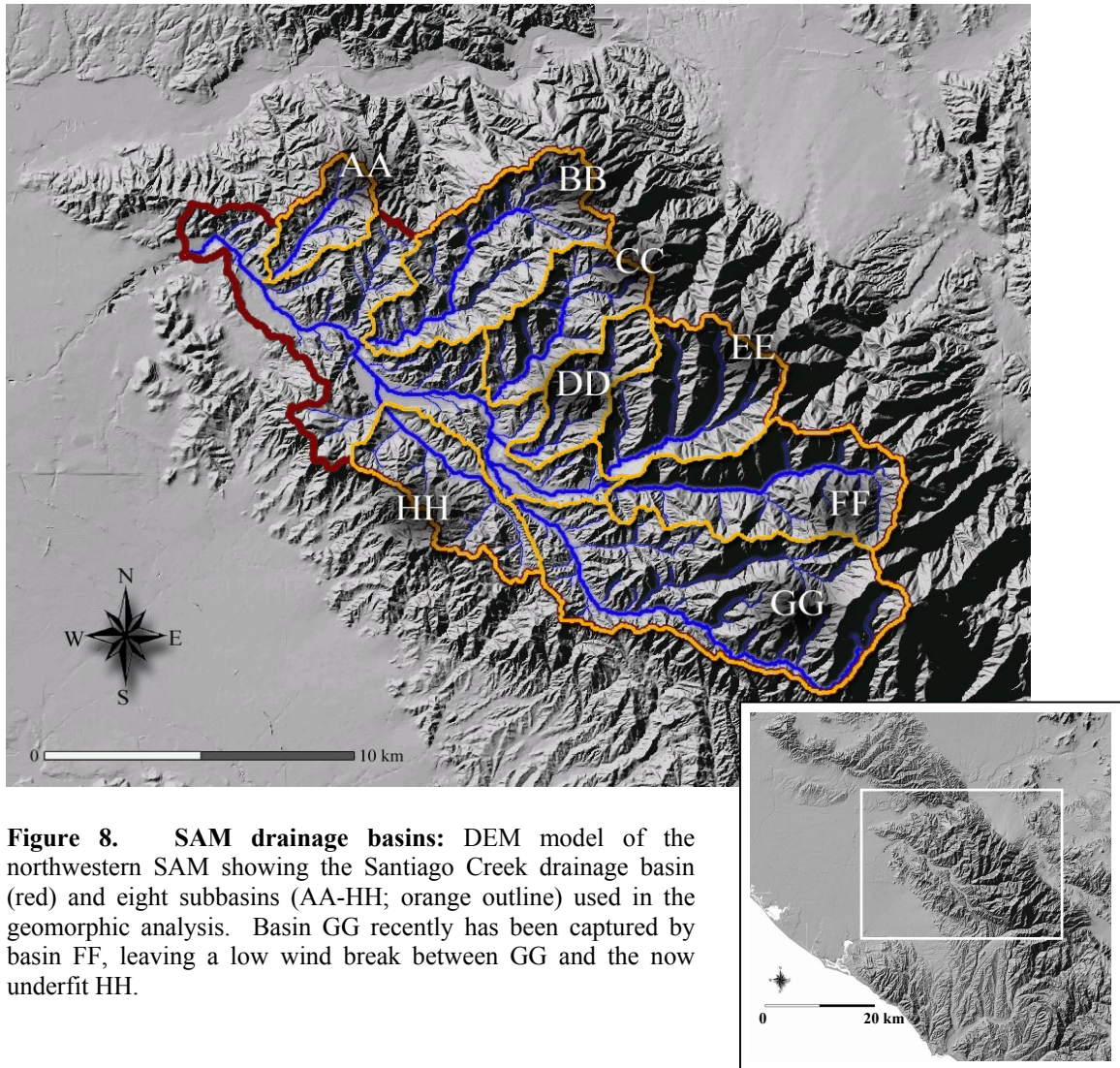


Figure 8. SAM drainage basins: DEM model of the northwestern SAM showing the Santiago Creek drainage basin (red) and eight subbasins (AA-HH; orange outline) used in the geomorphic analysis. Basin GG recently has been captured by basin FF, leaving a low wind break between GG and the now underfit HH.

Table 4. Eight Santa Ana Mountains drainage basins: area and age

Basin	Name	Area (km ²)	Age (ka)
AA	Weir	8.0	275
BB	Fremont	27.5	796
CC	Black Star	15.4	449
DD	Baker	12.3	373
EE	Ladd	21.5	614
FF	Silverado	26.8	774
GG	Santiago	48.7	1587
HH	Limestone	16.2	470

These data are used to plot Figure 11. Adding basin areas of GG and HH together partially reconstructs the area of basin GG prior to the capture of basin FF, which occurred relatively recently. Age derived as follows: $\text{age} = (0.2594)(\text{area})^2 + (17.526)(\text{area}) + 117.78$.

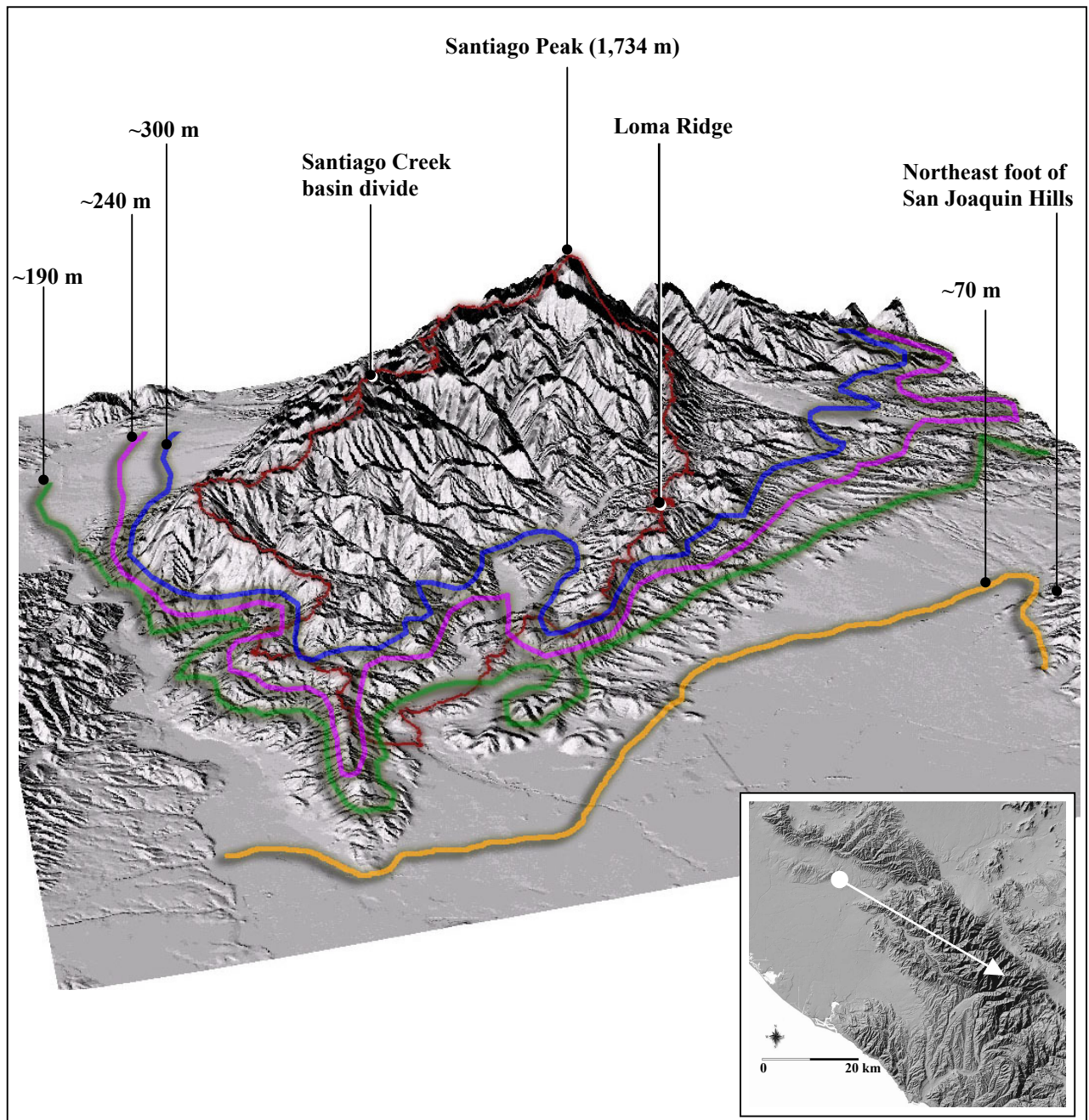


Figure 9. SAM geomorphic surfaces: This 3D oblique perspective is from the viewpoint of someone standing northwest of SAM looking southeast toward Santiago Peak (highest elevation in SAM). The boundary of the SAM drainage basin is outlined in red. Four geomorphic surfaces on Loma Ridge and the northern SAM are highlighted. The red, green, purple, and blue lines correspond to marine eustatic sea level high-stands as shown on Figure 10 (blue lines).

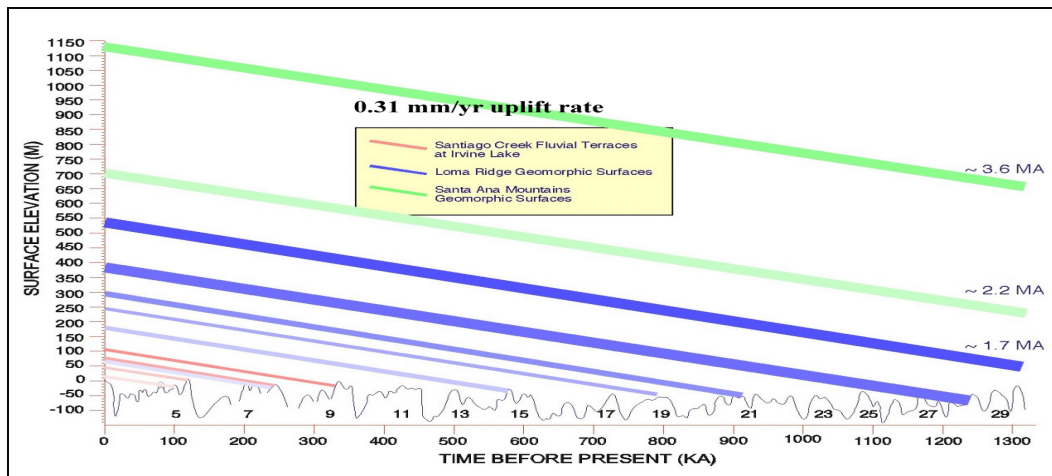


Figure 10. SAM geomorphic surfaces, elevation vs. eustatic sea level: Uplift rate plot of the fill terraces (red) and strath surfaces (blue and green) mapped on the northern SAM. The ages of the two youngest fill terraces (lightest red) were estimated from preliminary soil profile development in Santiago canyon. All other terraces were correlated to the eustatic marine sea level plot (Grant et al., 1999), assuming a constant uplift rate from those lowest terraces. Based on that assumption, the uplift of the SAM appears to have occurred at a rate of ~ 0.31 mm/yr, commencing ~ 3.6 Ma. Colors in this figure do not match colors in Figure 9. Line thickness indicates amount of uncertainty in elevation of surfaces.

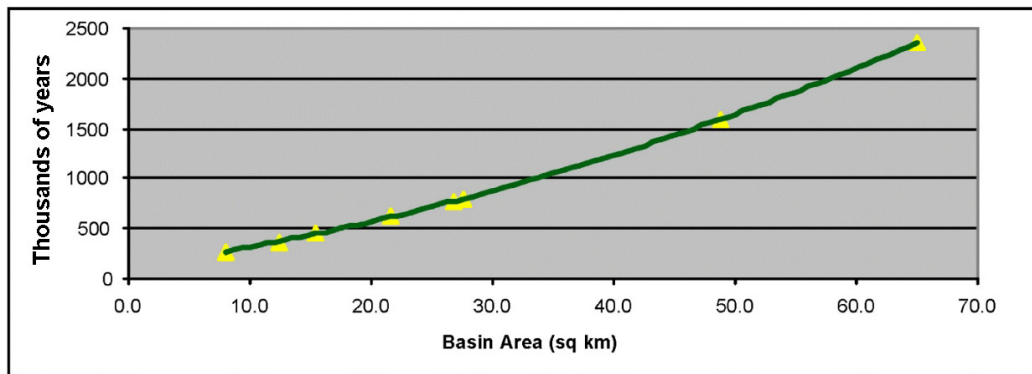
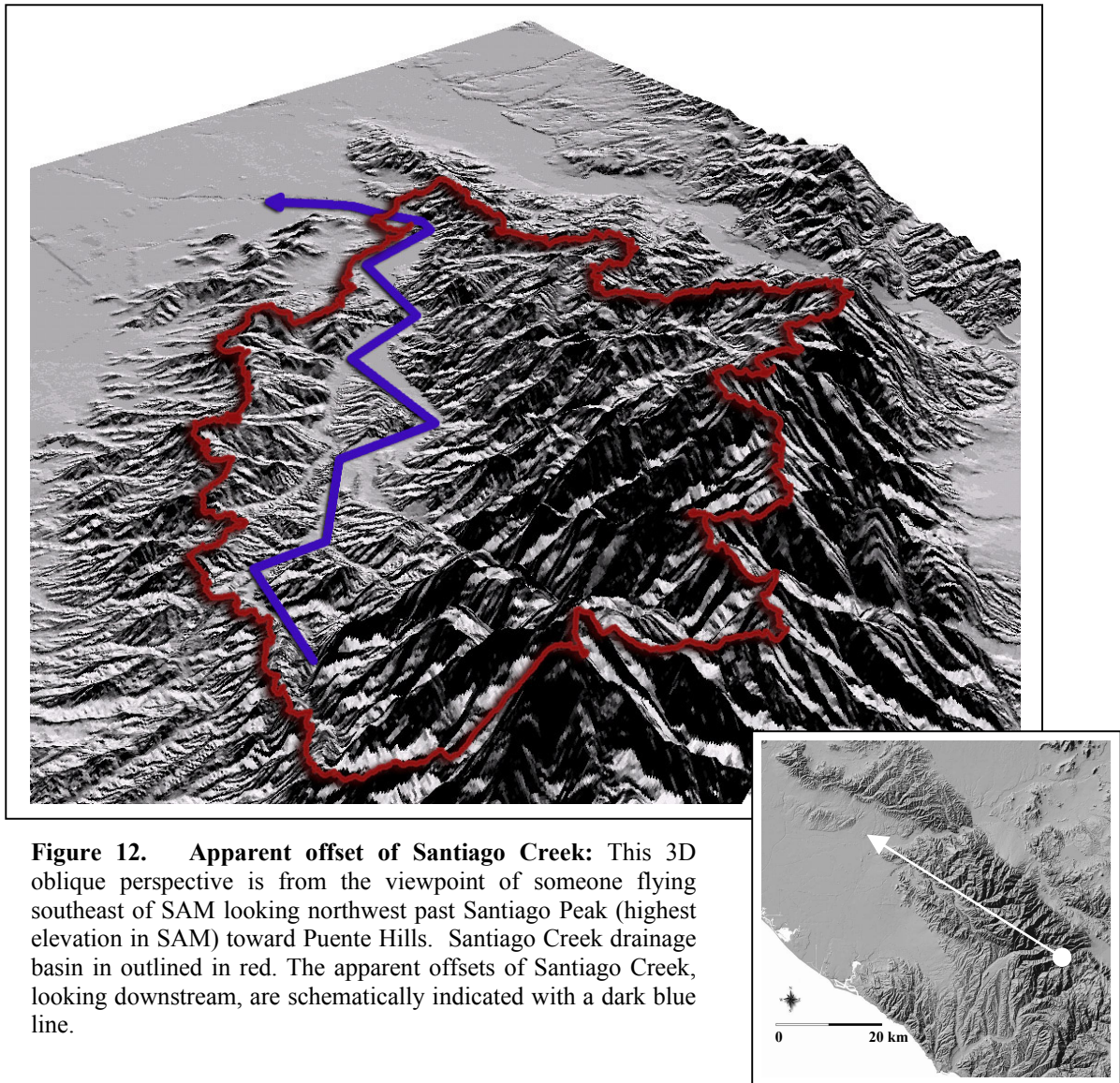


Figure 11. SAM, age vs. area: Graph shows the relationship between basin area (km^2) and basin age (thousands of years) calculated by applying the basin growth rate derived in the Puente Hills.

Santiago Creek is pinned against the north side of Loma Ridge by the progressive tilt of the Santa Ana block, as shown by the slip-off terraces on the north side of Santiago Creek (Figure 9); therefore, Loma Ridge must be relatively similar in age to the age of Santiago Creek. Based on Figure 11 and elevated geomorphic surfaces that cap its ridge, the age of Loma Ridge is estimated to be >2.4 Ma. Loma Ridge is additionally constrained because it is mantled on the south side by the Capistrano Oso sands, a recessional unit deposited as the Capistrano embayment filled. The Oso has been determined to be early Pleistocene to very early Pliocene in

age based on paleontological analysis (Stadum, 1984). This 2-3 Ma fossil age is consistent with the 2.4 Ma stream age determined from basin area relationships.

Santiago Creek appears to be deflected $\sim 1,200$ m northward (upstream) at a minimum of four locations (Figure 12). We propose two alternative explanations for the apparent upstream deflections. The first is that Loma Ridge episodically expands to the west, deforming Santiago Creek farther north and west as a result. Each increase in the western extent of Loma Ridge would need to be equivalent to the prior steps to account for the similarity in the deflections. This first explanation is unlikely because the rock-types differ non-uniformly. The second possibility is that the deflections are caused by a series of en-echelon fault blocks (see Figure 15), which right-laterally deform Santiago Creek. These fault blocks would be on the hanging wall of a blind thrust, accommodating the lateral strain from an oblique convergence. Assuming a 2.4 Ma age for Santiago Creek, each of the five fault blocks would accommodate 0.5 mm/yr of lateral strain. In this model, it is unclear whether the faults young to the west or all are acting in concert, yielding a 2.5 mm/yr slip rate across the system. Recent seismicity suggests activity of faults within the northern SAM block, but specific faults have not been identified.



HISTORIC SEISMICITY

The northern SAM are seismically active, as indicated by a series of three earthquakes ranging in magnitude from 3.5 to 4.0 (see Table 5, Figure 13) over a 17 month period beginning in December 1999. Figure 13 displays instrumental intensities for each mainshock. Felt intensities were recorded in Orange, Los Angeles, San Bernardino, Riverside and northern San Diego Counties. Preliminary focal mechanisms reported by TriNet included strike-slip and dip-slip solutions.

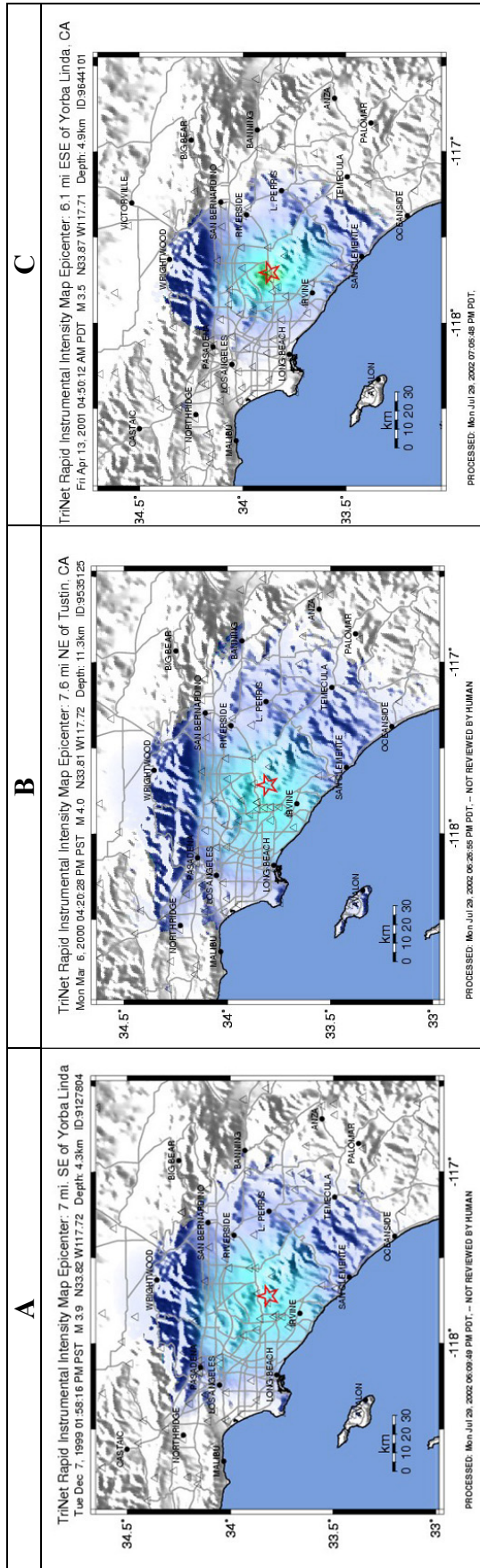
Microseismicity in the SAM has received relatively little investigation. Hull and Nicholson (1992) did a seismotectonic analysis of the northern Elsinore fault zone. Their study included analysis of microseismicity between 1979 and 1989. They modeled seismicity along the Elsinore fault and found that it deviated westerly of the fault's surface trace north of Lake Elsinore. Hull and Nicholson (1992) report several events under the northern SAM with reverse, thrust or oblique focal mechanisms. They inferred that the Glen Ivy North fault of the northern Elsinore fault zone changes strike to curve westward under the northern SAM, where it changes from a near vertical fault at Lake Elsinore to a shallow south-dipping fault near the Santa Ana River canyon.

PRELIMINARY TECTONIC MODEL

In this section we present a preliminary tectonic model to explain our observations from the first year of study. This model will be tested in the future with further analysis and data collection. Key elements of the model are shown in Figures 14 and 15.

SAM uplift is a result of the partial termination of the Elsinore fault in a leftward, compressional bend near the Santa Ana River canyon. North-vergent dextral strain (1.5 ± 0.5 mm/yr) is transferred to the Chino fault at Bedford Canyon, 15 km south of the Santa Ana River termination of the SAM structural block. North-vergent dextral strain (2.5 ± 0.5 mm/yr) is also transferred onto the Whittier fault 3-5 km south of the Santa Ana River, at a location where the Elsinore fault begins a progressively more pronounced change in structural style. At this location, the otherwise straight and steeply dipping Elsinore fault begins to dip more shallowly to the southwest and deflect more westerly in trend. It is this westerly deflection that is consuming the remaining 1-2 mm/yr of north-vergent strain, expressed topographically by the rapidly uplifting SAM.

Block faulting may be occurring due to strain partitioning on the hanging wall of the northern Elsinore thrust. It is driven by convergence with the Newport-Inglewood fault at a former step-over location, which was also responsible for the San Joaquin Hills uplift. It is uncertain whether these block faults are still active or whether the straightening of the Newport-Inglewood fault about 300-400 ka has removed them from the active strain field. In any event, they do not appear to offset the paleoshorelines along Loma Ridge.



Legend for maps A, B, and C

PERCEIVED SHAKING	Not felt	Weak	Light	Moderate	Strong	Very strong	Severe	Violent	Extreme
PGA (g)	none	none	1.4-3.9	3.9-9.2	9.2-16	18-34	34-65	65-124	>124
PEAK ACC (mg)	<.17	.17-1.4	1.4-3.9	3.9-9.2	9.2-16	18-34	34-65	65-124	>124
PEAK VEL (cm/s)	<0.1	0.1-1.1	1.1-3.4	3.4-8.1	8.1-16	16-37	37-60	60-116	>116
INSTRUMENTAL INTENSITY	I	II-III	IV	V	VI	VII	VIII	IX	X+

Figure 13. SAM vicinity ShakeMaps: Maps A, B, and C are based on ShakeMaps generated by TriNet, which are provided online (www.trinet.org). Red stars indicate locations of epicenters for recent earthquake events within the SAM vicinity. Cities and freeways provide reference points. Shades of green, blue, and purple represent instrumental intensity based on instrumental ground motion recordings to estimate Modified Mercalli Intensity maps

Table 5. Description of earthquakes

	A	B	C
Date	12-1999	3-2000	4-2001
Magnitude	3.9	4.0	3.5
Latitude	N33.82	N33.81	N33.87
Longitude	W117.72	W117.72	W117.71
Hypocentral depth	4.3 km	11.3 km	4.9 km

This table provides data associated with three earthquake illustrated in adjacent Figure 13.

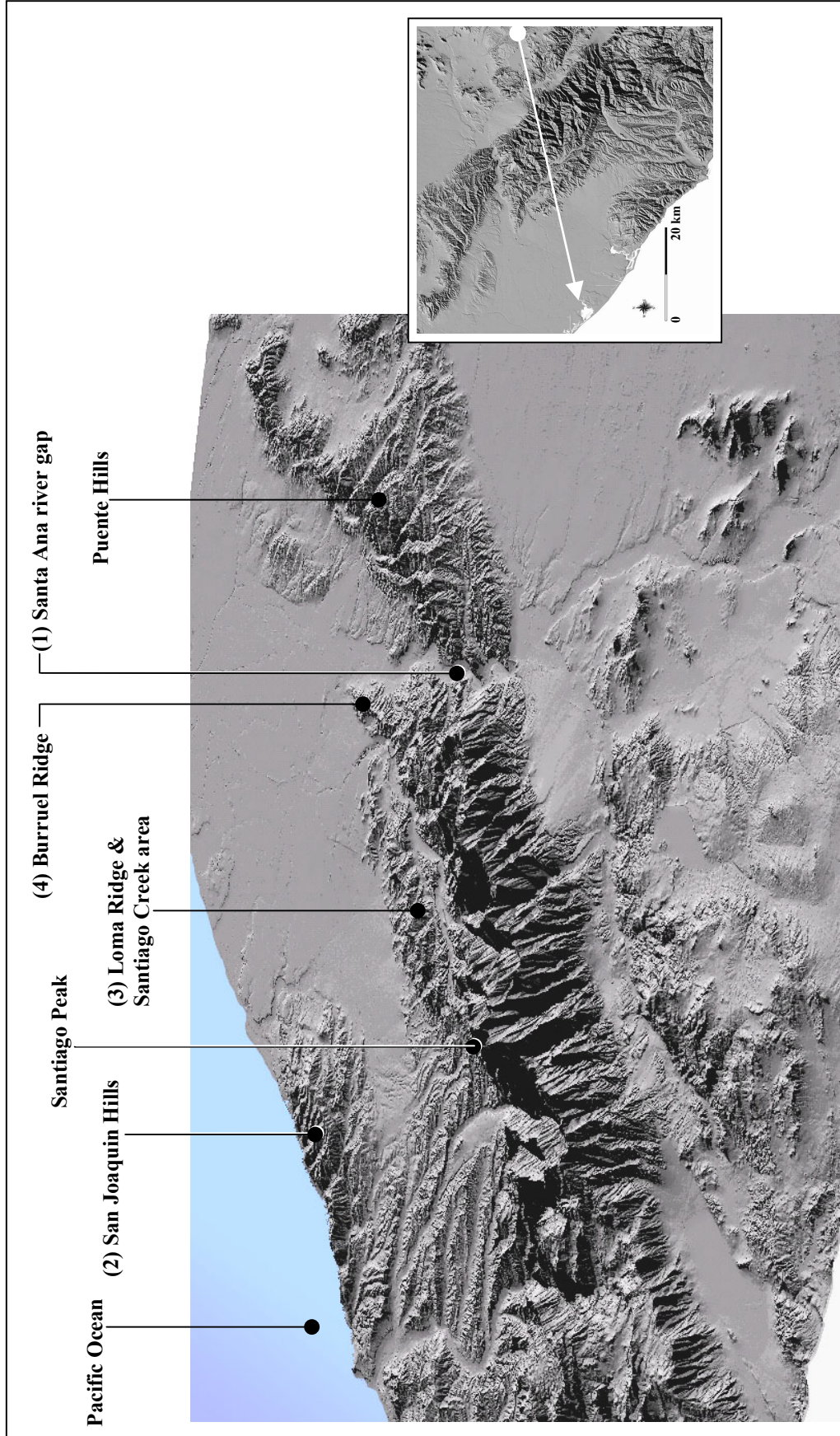


Figure 14. 3D oblique perspective of neotectonic model: Figure to illustrate our preliminary interpretation: (1) The uplift of the SAM and the Puente Hills periodically defeats the Santa Ana River's ability to maintain the water gap. As a result, sediments pond east of the mountain front. This model is similar to the effects observed by Meghraoui et al. (1988) from the El Asnam earthquake. (2) The pronounced north-south structural grain in southern Orange County is the result of north-vergent strain partitioned away from the Newport-Inglwood fault (NIF). Portions of this strain stepped westward returning to the NIF main trace. Consequently, a restraining bend produced the San Joaquin Hills (SJH). (3) A separate portion of the north-vergent strain (east of SJH) continued northward, resulting in an oblique convergence zone against the SAM. The strain was expressed as Loma Ridge being uplifted and multiple ~1,200 m deflections of Santiago Creek (also see Figure 12). (4) Westward growth of Burrel Ridge in the Peralta Hills is deflecting the Santa Ana River progressively westward. This structure is underlain by the Peralta Hills fault, which may be a backthrust from the Elsinore fault. The Elsinore has become a nearly pure reverse fault in the northwesternmost Peninsular Ranges.

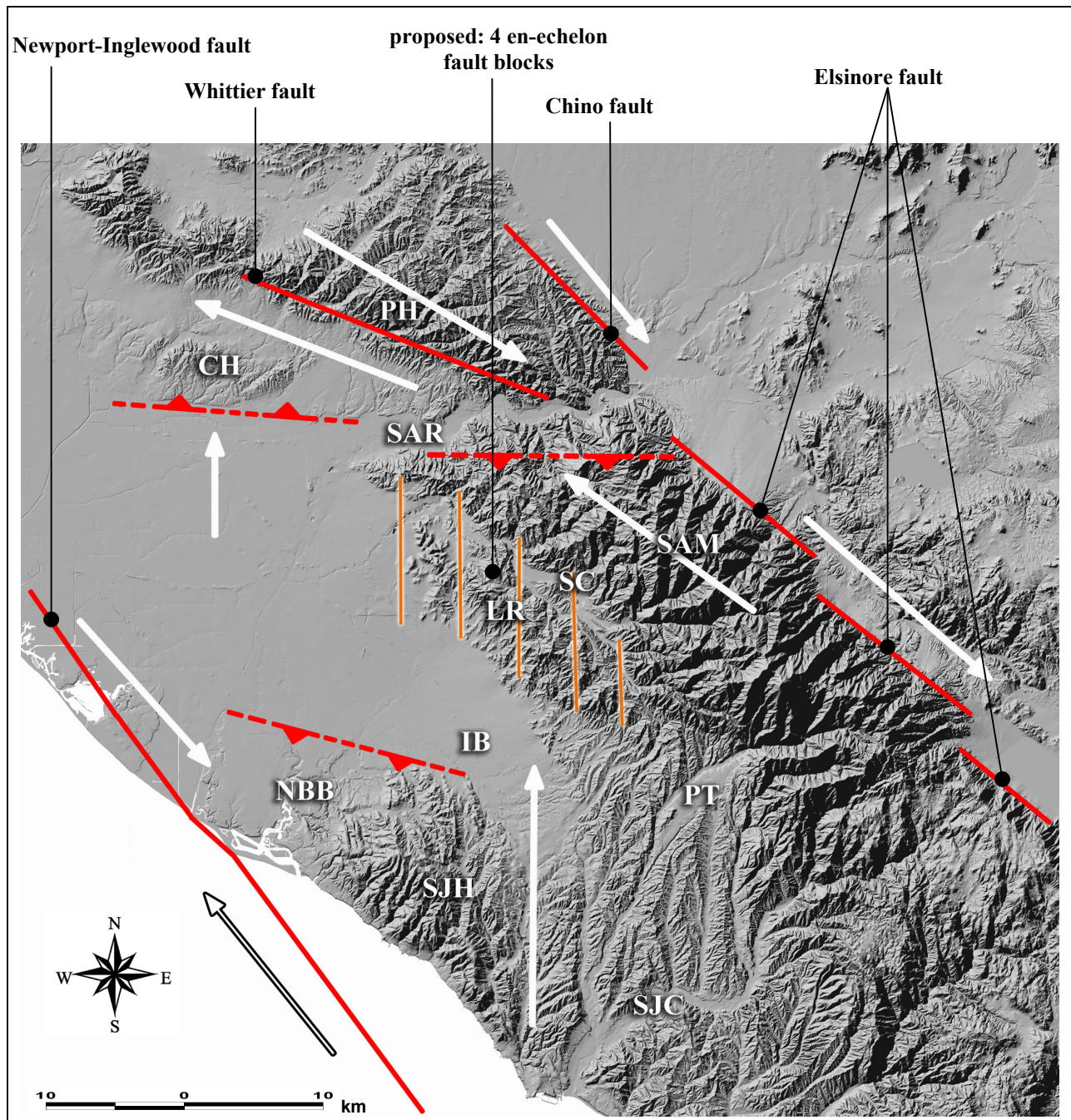


Figure 15. Neotectonic model: Proposed neotectonic model of the northern SAM and southern Los Angeles basin, Orange County, California. In this model, partitioned strain off the Newport-Inglewood fault causes uplift of the San Joaquin Hills (SJH). An underlying blind thrust fault (see Shearer and Shaw, 2000) causes uplift of the Puente Hills (PH) and Coyote Hills (CH). The SAM uplift is caused by a partial termination of the Elsinore fault and consumption of slip along a north-vergent blind thrust aligned roughly east-west. The Loma Ridge (LR) uplift is caused by north-vergent strain that is compressing the Tertiary sediments against the uplifting SAM, forming Loma Ridge and deforming Santiago Creek (SC) trapped between them. Arrows indicate direction of motion. Solid red lines are previously mapped strike-slip faults. Dashed red lines are suspected blind thrust faults. Our proposed en-echelon faults are indicated by five orange lines.

REFERENCES

- Bryant, M.E. & Fife, D.L. (1992). The Peralta Hills fault, a Transverse Ranges structure in the northern Peninsula Ranges, southern California. in Fife, D.L. & Minch, J.A. (eds), *Geology and Mineral Wealth of the California Transverse Ranges*. South Coast Geological Society, Santa Ana, California, p. 403-409.
- Bullard, T.F. & Lettis, W.R. (1993). Quaternary fold deformation associated with blind thrust faulting, Los Angeles basin, California. *Journal of Geophysical Research*, 98 (B5), 8349-8369.
- Cox, R.T. (1994). Analysis of drainage basin symmetry as a rapid technique to identify areas of possible Quaternary tilt-block tectonics: An example from the Mississippi Embayment. *Geological Society of America Bulletin*, 106, 571-581.
- Durham, D.L. & Yerkes, R.F. (1964). Geology and oil resources of the eastern Puente Hills area, southern California. *U.S. Geological Survey Professional Paper 420-B*, 62 p.
- Fife, D.L., (1974). Geology of the south half of the El Toro quadrangle, Orange County, California. *California Geological Survey Special Report 110*, 27 p.
- Gath, E.M., Gonzalez, T., & Rockwell, T.K. (1992). Evaluation of the late Quaternary rate of slip, Whittier fault, southern California. *USGS Final Technical Report, NEHRP Contract No. 14-08-0001-G1696*, 24 p., numerous plates.
- Gath, E.M. (1997). Tectonic geomorphology of the eastern Los Angeles Basin. *USGS Final Technical Report, NEHRP Contract No. 1434-95-G-2526*, 13 p., 1 plate, 6 figures, 6 tables.
- Grant, L.B., Mueller, K.J., Gath, E.M., Cheng, H., Edwards, R.L., Munro, R., & Kennedy, G.L. (1999). Late Quaternary uplift and earthquake potential of the San Joaquin Hills, southern Los Angeles basin, California. *Geology*, 27, 1031-1034.
- Grant, L.B., Mueller, K.L., Gath, E.M., & Munro, R. (2000). Late Quaternary uplift and earthquake potential of the San Joaquin Hills, southern Los Angeles basin, California – REPLY, *Geology*, 28, (4), 384.
- Grant, L.B., Ballenger, L.J., & Runnerstrom, E.E. (2002). Evidence of a large earthquake and coastal uplift of the San Joaquin Hills, southern Los Angeles basin California, since 1635 A.D. *Bulletin of Seismological Society of America*, 92, (2), 590-599.
- Hack, J.T. (1973). Stream-profile analysis and stream-gradient index. *U.S. Geological Survey Journal of Research*, 1, 421-429.
- Heath, E.G., Jensen, D.E., & Lukesh, D.W. (1982). Style and age of deformation on the Chino fault: in Cooper, J.D. (ed.), *Neotectonics in southern California: Geological Society of America Cordilleran Section, Field Trip Guidebook*, 123-134.
- Hull, A.G. & Nicholson, C. (1992). Seismotectonics of the northern Elsinore fault zone, southern California. *Bulletin of the Seismological Society of America*, 82, (2), 800-818.
- Kirby, E. & Whipple, K. (2001). Quantifying differential rock-uplift rates via stream profile analysis. *Geology*, 29, 415-418.
- Lamar, D.L. & Rockwell, T.K. (1986). An overview of the tectonics of the Elsinore fault zone; in Ehlig, P.L. (ed.), *Neotectonics and faulting in southern California, Geological Society of America Cordilleran Section, Field Trip Guidebook*, 149-158.
- Meghraoui, M., Philip, H., Albaredo, F., & Cisternas, A. (1988). Trench investigations through the trace of the 1980 El Asnam thrust fault: evidence for paleoseismicity. *Bulletin of Seismological Society of America*, 78, (2), 979-999.

- McGill, S.F. & Sieh, K. (1991). Surficial offsets on the central and eastern Garlock fault associated with prehistoric earthquakes. Journal of Geophysical Research, 96, (B13), 21,597-21,621.
- Mendenhall, W.C. (1905). Development of underground waters in the eastern coastal plain region of southern California. U.S. Geological Survey Water-Supply Paper 137, 140 p.
- Merritts, D.J., Vincent, K.R., & Wohl, E.E. (1994). Long river profiles, tectonism, and eustasy: A guide to interpreting fluvial terraces. Journal of Geophysical Research, 99, (B7), 14,031-14,050.
- Montgomery, D.R. (1994). Valley incision and the uplift of mountain peaks. Journal of Geophysical Research, 99, 13,913-13,921.
- Morton, P.K. & Miller, R.V. (1981). Geologic map of Orange County, California showing locations of mines and mineral deposits. California Division of Mines and Geology Bulletin 204, 1:48,000.
- Nicol, A., Alloway, B., & Tonkin, P. (1994). Rates of deformation, uplift, and landscape development associated with active folding in the Waipara area of North Canterbury, New Zealand. Tectonics, 13, 1327-1344.
- Ohmori, H. (1993). Changes in the hypsometric curve through mountain building resulting from concurrent tectonics and denudation. Geomorphology, 8, 263-277.
- Pazzaglia, F.J., Gardner, T.W., & Merritts, D.J. (1998). Bedrock fluvial incision and longitudinal profile development over geologic time scales determined by fluvial terraces: Rivers over Rock - Fluvial Processes in Bedrock Channels. American Geophysical Union, Geophysical Monograph, 107, 207-235.
- Rivero, C., Shaw, J. H. & Mueller, K. (2000). Oceanside and Thirty-mile Bank blind thrusts: Implications for earthquake hazards in coastal southern California, Geology, 28, (10), 891-894.
- Rockwell, T.K., Gath, E.M., & Cook, K.D. (1988). Sense and rate of slip on the Whittier fault zone near Yorba Linda, California (abs.). Abstracts with Programs, Cordilleran Section, Geological Society of America, 20, (3), 224.
- Rockwell, T.K., Gath, E.M., & Gonzalez, T. (1992). Sense and rate of slip on the Whittier fault zone, eastern Los Angeles basin, California. in Stout, M.L. (ed), Proceedings of the 35th Annual Meeting, Association of Engineering Geologists, 679.
- Rosenbloom, N.A., & Anderson, R.S. (1994). Hillslope and channel evolution in a marine terraced landscape, Santa Cruz, California. Journal of Geophysical Research, 99, 14,013-14,029.
- Ryan, J.A., Burke, J.N., Walden, A.F., & Wieder, D.P. (1982). Seismic refraction study of the El Modena fault, Orange County, California. California Geology, January, 15-19.
- Schoellhamer, J.E., Vedder, J.G., Yerkes, R.F., & Kinney, D.M. (1981). Geology of the northern Santa Ana Mountains, California. U.S. Geological Survey Professional Paper 420-D, 109 p.
- Schumm, S.A. (1986). Alluvial river response to active tectonics, in Studies in National Research Council (eds), Active Tectonics. National Academy Press, Studies in Geophysics, Washington, D.C., 80-94.
- Schumm, S.A., Mosley, M.P., & Weaver, W.E. (1987). Experimental fluvial geomorphology: John Wiley & Sons, New York, 413 p.
- Shaw, J.H. & Shearer, P.M. (1999). An elusive blind-thrust fault beneath metropolitan Los Angeles. Science, 283, 1516-1518.

- Stadum, C.J. (1984). The fossils of the Niguel Formation of southeastern Orange County. The Natural Sciences of Orange County, Natural History Foundation Memoir, 1, 76-83.
- Weber, F.H. Jr. (1977). Seismic hazards related to geological factors, Elsinore and Chino fault zones, northwestern Riverside County, California. California Division of Mines and Geology Open File Report 77-4-LA.
- Whitney, R.A. & Seymour, D.C. (1992). Active strike-slip faulting within the Peralta Hills anticline, Orange County, California—a Transverse Range-Peninsula Range boundary. American Association of Petroleum Geologists, 76, 432.
- Wohl, E.E. (1998). Bedrock channel morphology in relation to erosional processes; Rivers over Rock: Fluvial Processes in Bedrock Channels. American Geophysical Union, Geophysical Monograph, 107, 133-151.
- Yerkes, R.F. (1972). Geology and oil resources of the western Puente Hills area, southern California. U.S. Geological Survey Professional Paper 420-C, 63 p.

BIBLIOGRAPHY OF PUBLICATIONS RESULTING FROM WORK PERFORMED

- Gath, E.M. & Grant, L.B. (2002). Is the Elsinore fault responsible for the uplift of the Santa Ana Mountains, Orange County, California (abs.). Abstracts with Programs, 98th Annual Meeting, Cordilleran Section, Geological Society of America, 34, (5), A-87.

Appendix: Description of USGS 7.5-minute digital elevation model quadrangles used to map study area and vicinity

Name of USGS 7.5-minute digital elevation model quadrangle	elevation units	horizontal resolution (m)	Star (*) indicates use in Puente Hills coverage area	Star (*) indicates use in Santa Ana Mountains coverage area
Alberhill	feet	10		*
Anaheim	feet	10		
Baldwin Park	feet	10		
Black Star Canyon	feet	10	*	*
Canada Gobernadora	feet	10		
Corona North	meters	10		*
Corona South	feet	10		*
Dana Point	meters	10		
El Monte	meters	10		
El Toro	feet	10		*
Fallbrook	feet	10		
Fontana	meters	10		
Guasti	meters	10		
La Habra	feet	10	*	
Laguna Beach	feet	10		
Lake Elsinore	feet	10		
Lake Mathews	feet	10		*
Los Alamitos	feet	10		
Margarita Peak	meters	30		
Newport Beach OE S	feet	10		
Newport Beach	feet	10		
Ontario	feet	10	*	
Orange	feet	10	*	*
Prado Dam	feet	10	*	*
Riverside East	feet	10		
Riverside West	meters	10		
San Bernardino South	feet	10		
San Clemente	meters	10		
San Dimas	feet	10	*	
San Juan Capistrano	feet	10		
Santiago Peak	feet	10		*
Seal Beach	feet	10		
Sitton Peak	feet	10		
Steele Peak	feet	10		
Tustin	feet	10		*
Whittier	feet	10		
Wildomar	feet	10		
Yorba Linda	feet	10	*	*